Memorandum

November 16, 2021

TO: WECC Modeling and Validation Subcommittee (MVS) and Renewable Energy Modeling Working Group (REMWG)

FROM: Deepak Ramasubramanian, EPRI; dramasubramanian@epri.com
CC: Anish Gaikwad, Evangelos Farantatos, EPRI; Brian Johnson, UW; Sairaj Dhople, UMN; Olaoluwapo Ajala, Alejandro Dominguez-Garcia, UIUC; Pouyan Pourbeik, PEACE®

SUBJECT: **PROPOSAL FOR GENERIC GRID FORMING (GFM) POSITIVE SEQUENCE MODEL**

This document describes a proposal for a generic grid forming (GFM) inverter-based resource (IBR) positive sequence model. The development of this model is based on research work carried jointly across EPRI, University of Washington (UW), University of Illinois Urbana Champaign (UIUC), and University of Minnesota (UMN). Associated research results and further details are available in references [1] [2] [3] [4] [5].

The generic GFM model can represent, in a general way, four different types of GFM control methods that have been proposed in the literature. These methods are:

1. Droop based GFM
2. Virtual Synchronous Machine (VSM) based GFM
3. Dispatchable Virtual Oscillator (dVOC) based GFM
4. Phase Locked Loop (PLL) based GFM

An underlying structural similarity across the first three methods [1] [2] forms the basis for this generic model while an operational similarity with the fourth method [4] [5] completes the model to allow it to cater to a wide variety of different IBR control representations. In the following sections, the specifications of the model along with its parameters will first be provided followed by testing and validation results.

Model specification

The generic GFM model can be structured in a modular fashion like the existing WECC generic model suite as shown in Figure 1 and Figure 2. In these figures, variables in blue color indicate input variables from the network to the control structure, orange color indicates output variables from the control structure to the network, green color indicates variables that can pass between different models, purple color indicates input reference values, and red color indicates state variables. All other variables are either local variables or control gains/flag settings. The *xy* reference frame is the real – imaginary coordinate frame of the network while the *dq* reference frame is the coordinate frame of the control. The relative angle between these reference frames is denoted by the control variable θ_{inv}.

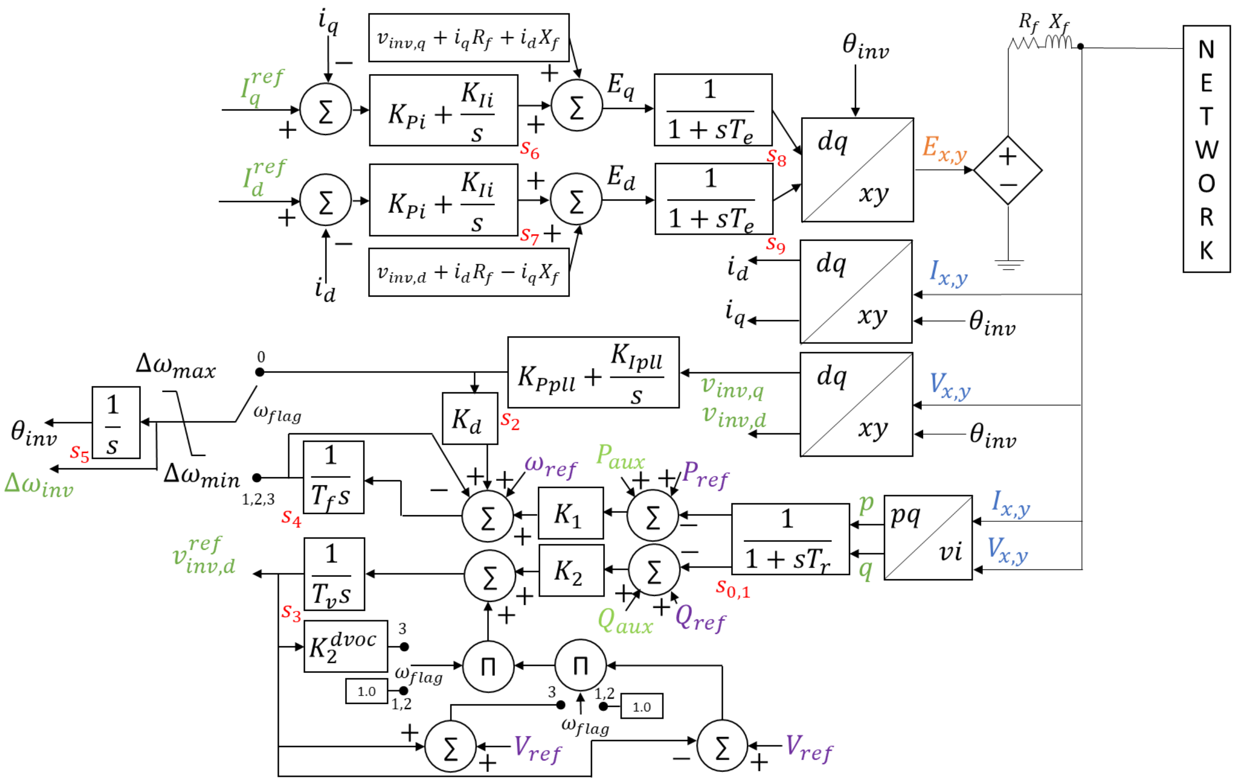

Figure 1: Generic grid forming (GFM) renewable generator/converter (REGC_*) model

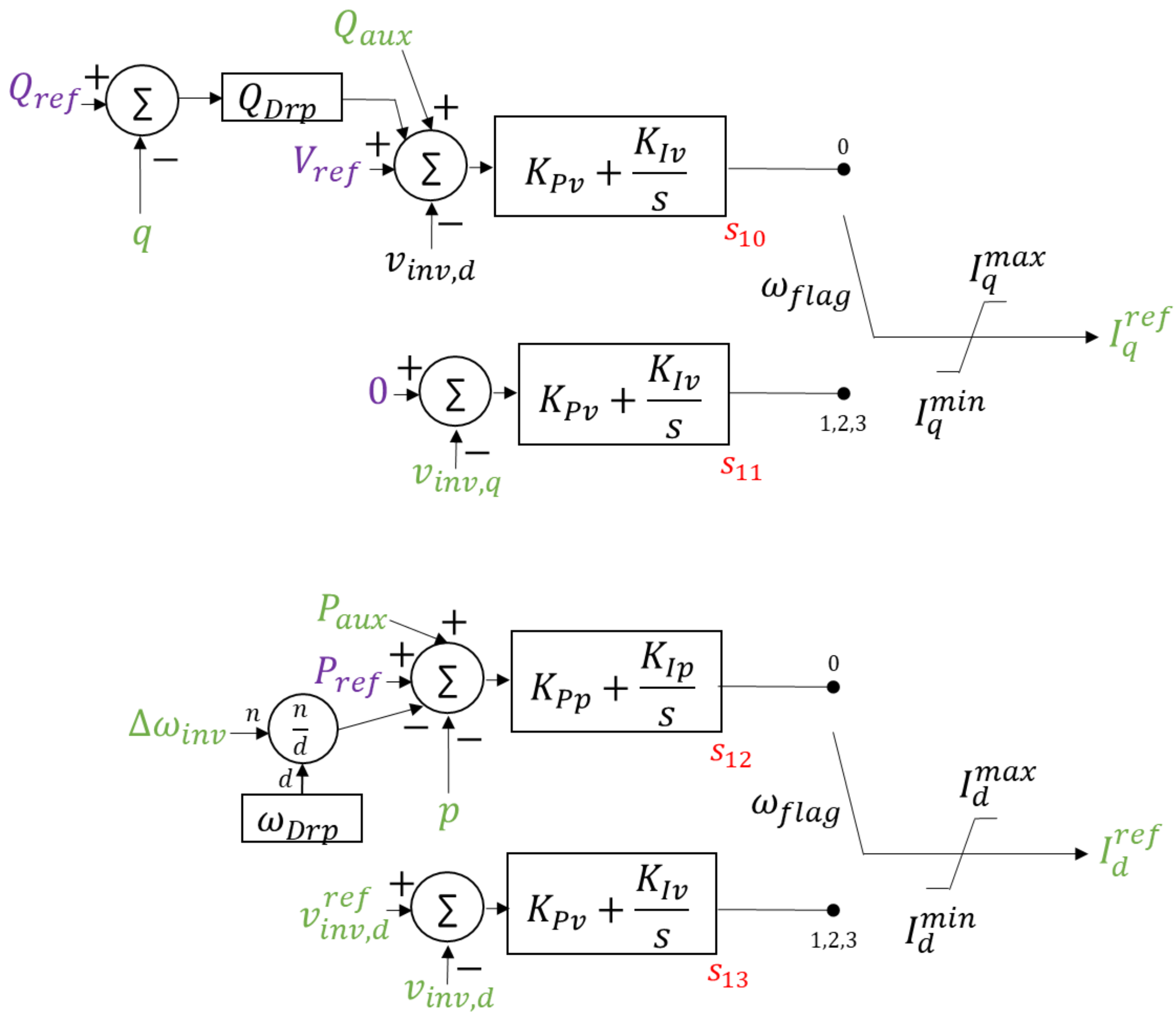

Figure 2: Generic grid forming (GFM) renewable electrical control (REEC_*) model

Due to the generalized nature of the model, not all control gains shown in the figures are direct inputs from the user. The inputs from the user for the independent parameters are tabulated in Table 1 while the values of the dependent parameters (i.e., the parameters derived from the user inputs based on the type of GFM control method chosen) are as tabulated in Table 2.

Table 1: Input parameters entered by the user for the generic GFM model

Parameter	Description	Units	Default Value
MVA rating	IBR rating	MVA	100.0
R_f	Filter resistance	pu on MVA rating	0.0015
X_f	Filter reactance	pu on MVA rating	0.15
V_{dip}	State freeze threshold	pu	0.8

I_{max}	Maximum current magnitude	pu	1.2
PQflag	Current priority	-	0 – P priority 1 – Q priority
ω_{flag}	GFM control type	-	0 – PLL based GFM 1 – Droop based GFM 2 – VSM based GFM 3 – dVOC based GFM
$\Delta\omega_{max}$	Maximum value of frequency deviation	rad/s	75.0
$\Delta\omega_{min}$	Minimum value of frequency deviation	rad/s	-75.0
ω_{drp}	Frequency droop percent	-	0.033
Q_{drp}	Voltage droop percent	-	0.045
T_r	Transducer time constant	s	0.005
T_e	Output state time constant	s	0.01
m_f	VSM inertia constant	-	0.15
d_d	VSM damping factor	-	0.11
K_{Ppll}	PLL proportional gain	-	20.0
K_{Ipll}	PLL integral gain	-	700.0
K_{Pi}	Current control proportional gain	-	0.5
K_{Ii}	Current control integral gain	-	20.0
K_{Pv}	Voltage control proportional gain	-	0.5 (if $\omega_{flag} = 0$) 3.0 (if $\omega_{flag} \neq 0$)
K_{Iv}	Voltage control integral gain	-	150.0 (if $\omega_{flag} = 0$) 10.0 (if $\omega_{flag} \neq 0$)
K_{Pp}	Active power proportional gain	-	0.5
K_{Ip}	Active power integral gain	-	20.0

Table 2: Values of dependent parameters based on user input parameters

GFM Control Type	$\boldsymbol{T_f}$	$\boldsymbol{T_v}$	$\boldsymbol{K_d}$	$\boldsymbol{K_1}$	$\boldsymbol{K_2}$	$\boldsymbol{K_2^{dvoc}}$
PLL based	N/A	N/A	0.0	N/A	N/A	N/A
Droop based	0.0	0.0	0.0	ω_{drp}	Q_{drp}	N/A
VSM based	$m_f{*}\omega_{drp}$	0.0	$d_d{*}\omega_{drp}$	ω_{drp}	Q_{drp}	N/A
dVOC based	0.0	$1.0/\omega_0$	0.0	$\omega_{drp}/(s_3)^2$	ω_{drp}/s_3	*eqn (1)*

The value of K_2^{dvoc} is evaluated as,

$$\frac{K_2^{dvoc}}{\omega_{drp}} = \frac{4 * 100^4}{100^4 - \left(2 * \left(100 - 100 * Q_{drp}\right)^2 - 100^2\right)^2} \quad (1)$$

Here, parameters ω_{drp} and Q_{drp} are the values of droop, however not expressed in percent. For example, an ω_{drp} of 5% will be represented as 0.05. In the model, all input reference values (purple colored variables) are specified in per unit on the MVA and kV rating of the IBR device. Further, input variables (blue colored variables) and output variables (orange colored variables) are also in per unit on the rating of the IBR device. It is expected that each software environment will handle the corresponding per unit conversions between the device and the network. Additionally, the network interface is modeled as a voltage source in a manner which is like the REGC_C model [6]. Due to the voltage source nature of the interface, there could also be a need to ensure current limits are maintained during a fault. This can require an algebraic iteration with the network solution at each time step during the fault. The method adopted in the REGC_C model and explained in detail in [6] [7] is also adopted in this model. Additionally, if needed, a shunt capacitor filter can be added on the grid side of X_f and its associated equations can be used in the determination of I_d^{ref} and I_q^{ref}.

The model also has the capability to receive signals P_{aux} and Q_{aux} from auxiliary control modules such as power oscillation dampers, automatic generation control blocks, plant controllers, etc. Additionally, when terminal voltage magnitude (i.e., $\sqrt{v_{inv,d}^2 + v_{inv,q}^2}$) falls below the freeze threshold V_{dip}, states $s_2, s_{10}, s_{11}, s_{12}, s_{13}$ are frozen.

Further, it can be noticed that the layout of the PLL based GFM mode option is like the existing REGC_C + REEC_D + REPC_A models. A detailed explanation of the use of the REGC_C + REEC_D + REPC_A models in grid forming mode (for non-blackstart scenarios) is provided in reference [8].

Commentary on use of inner current control loop

An inner current control loop is utilized to control the output current of the inverter and limit its value to a desired range of values, which are based on the inverter ratings. The control loop takes as its reference a desired output current of the inverter and uses it to compute voltage setpoints for the three-phase inverter. This results in the inverter operating as a signal-controlled voltage source. Such a grid forming control structure is often referred to as a multi-loop grid forming method.

Benchmarking of positive sequence generic model dynamic behavior against generic EMT model

The working of the proposed generic GFM positive sequence model has been benchmarked against a corresponding model developed in EMT domain. The positive sequence model has been developed in GE-PSLF™ while the EMT model has been developed in PSCAD. EMT domain simulations are carried out at a time step of 5µs while positive sequence simulations are carried out a time step of 1ms.

To benchmark the model behavior, first a single inverter connected to an equivalent voltage source is considered. The setup of the network is as shown in Figure 3. At the start of the simulation the inverter is dispatched with $P_{ref} = 800MW$ and $V_{ref} = 1.035pu$ along with $P_{load} = 900MW$ and $Q_{load} = 210Mvar$. Since the dispatch of the IBR is lower than the total load, the surplus power is provided by the equivalent voltage source. At *t=5.0s* the breaker connecting the equivalent source to the rest of the circuit is opened thereby creating a 100% inverter network. Following this at *t=10.0s* a solid to ground three phase fault is applied at the POI.

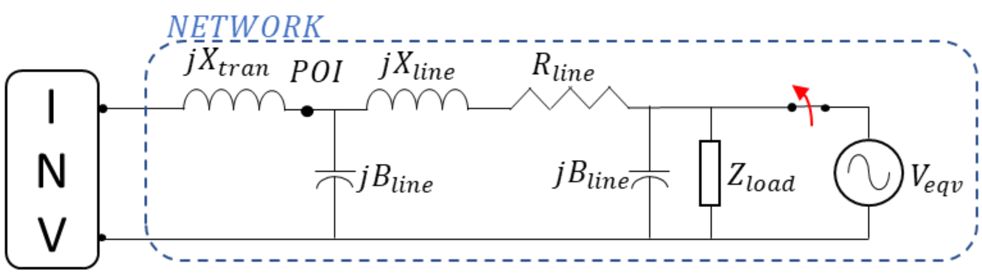

Figure 3: Single inverter-load-equivalent voltage source network to benchmark positive sequence model behavior

A comparison of the response in EMT domain across all four grid forming modes of the model is shown in Figure 4 while a comparison of the response across all four grid forming modes in positive sequence domain is shown in Figure 5. From both figures the similarity of the responses can be observed.

A one-to-one comparison of the behavior of the dVOC GFM mode across both EMT domain and positive sequence domain is shown in Figure 6. When the equivalent source is disconnected, initially there is a deficit in generation in the network as the IBR resource was dispatched at 800 MW. The deficit in generation both from active and reactive power results in voltage and frequency dropping. Subsequently, in all grid forming modes, frequency and voltage is controlled with an increase in active power and reactive power output. The response for a subsequent three phase solid to ground fault is also shown. It is seen that across all grid forming modes, both in EMT domain or positive sequence domain, the response of the generic model is similar and consistent with seamless translation of parameter values.

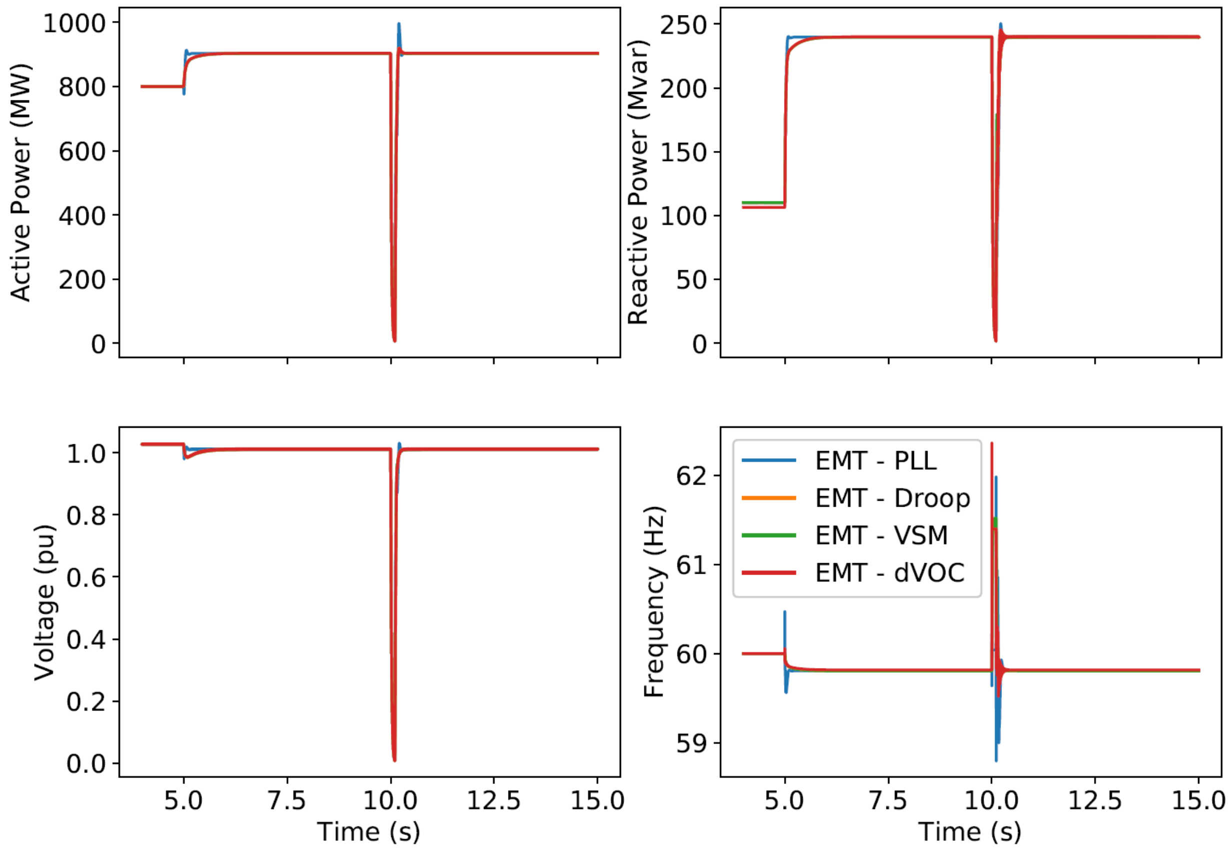

Figure 4: Comparison of EMT time domain response of the generic model in different GFM modes

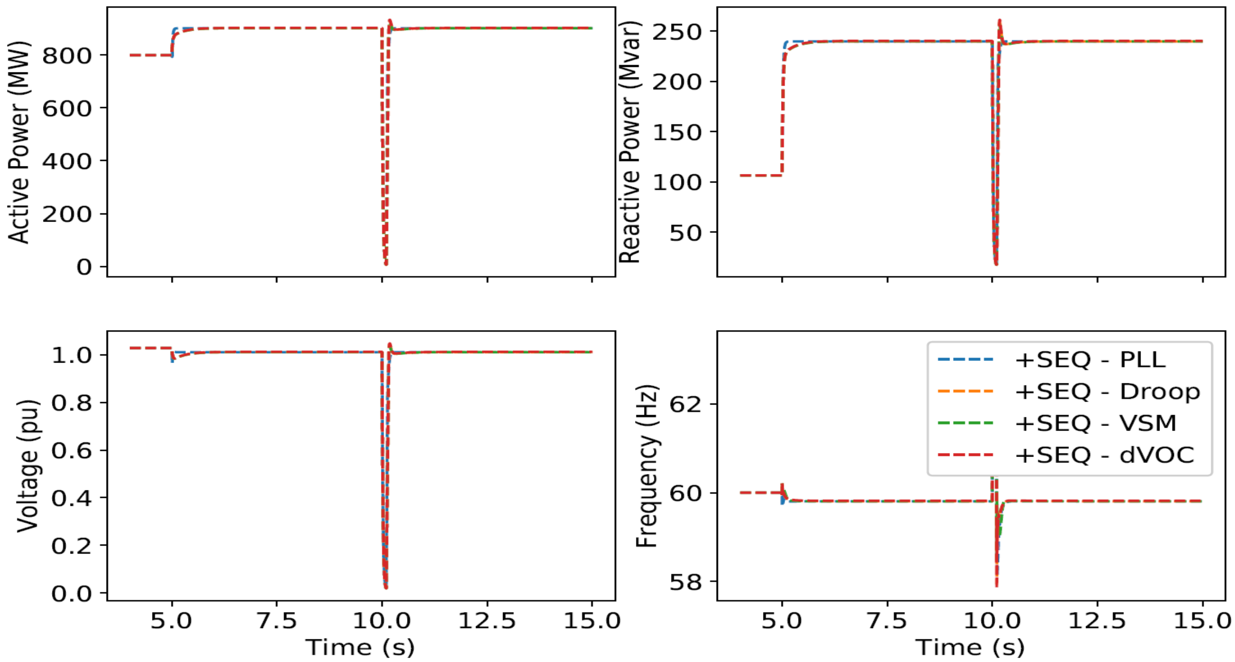

Figure 5: Comparison of positive sequence time domain response of the generic model in different GFM modes

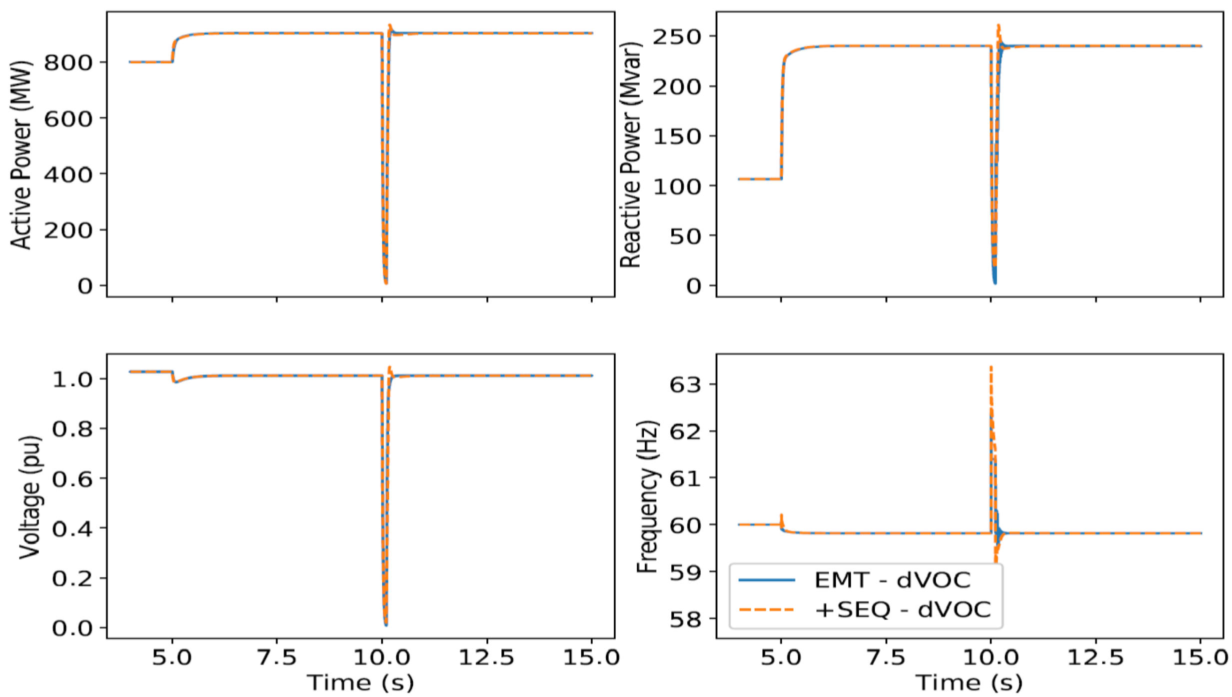

Figure 6: Comparison of EMT domain and positive sequence time domain response of the generic model in dVOC GFM mode

To extend the comparison to a multi-inverter resource system with different control types the IEEE 14 bus benchmark system topology is used with a few modifications as shown in Figure 7. The response across both positive sequence domain and EMT domain to two consecutive load events at Bus 14 is shown in Figure 8. The comparison of response to multiple line outages followed by two consecutive three phase to ground solid faults is shown in Figure 9.

Both comparison results showcase the fidelity and robustness of the proposed generic positive sequence model in being able to replicate the dynamic behavior of the grid forming devices.

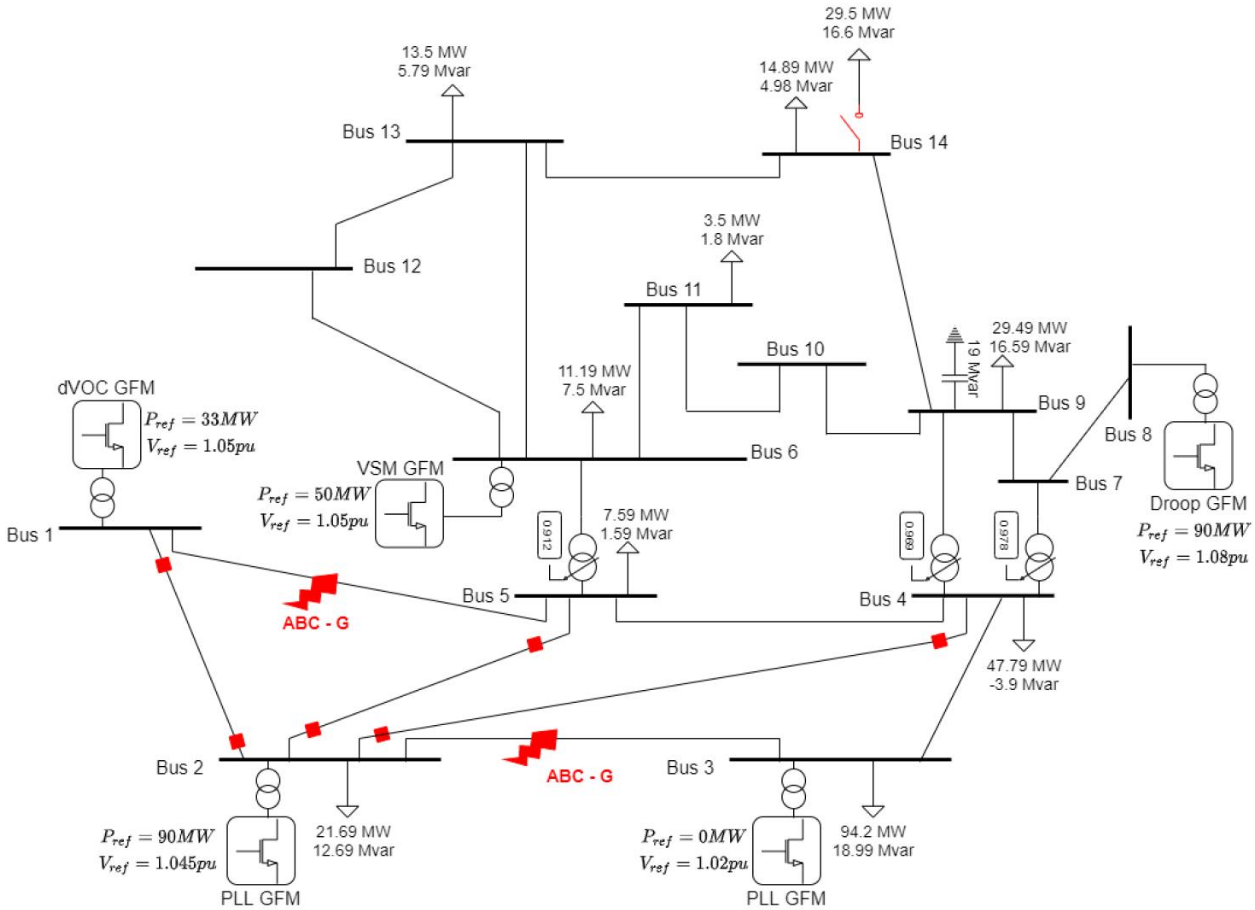

Figure 7: IEEE 14 bus benchmark system topology to benchmark model behavior with multiple IBR sources

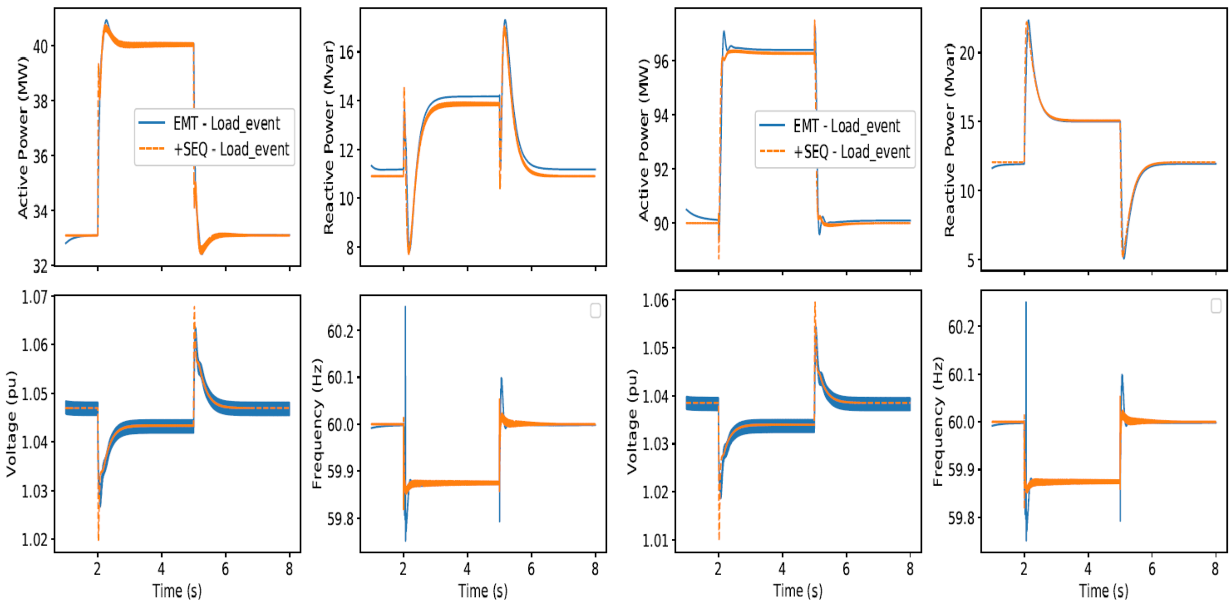

Figure 8: Behavior of IBR at bus 1 (left) and IBR at bus 2 (right) in response to two consecutive load events

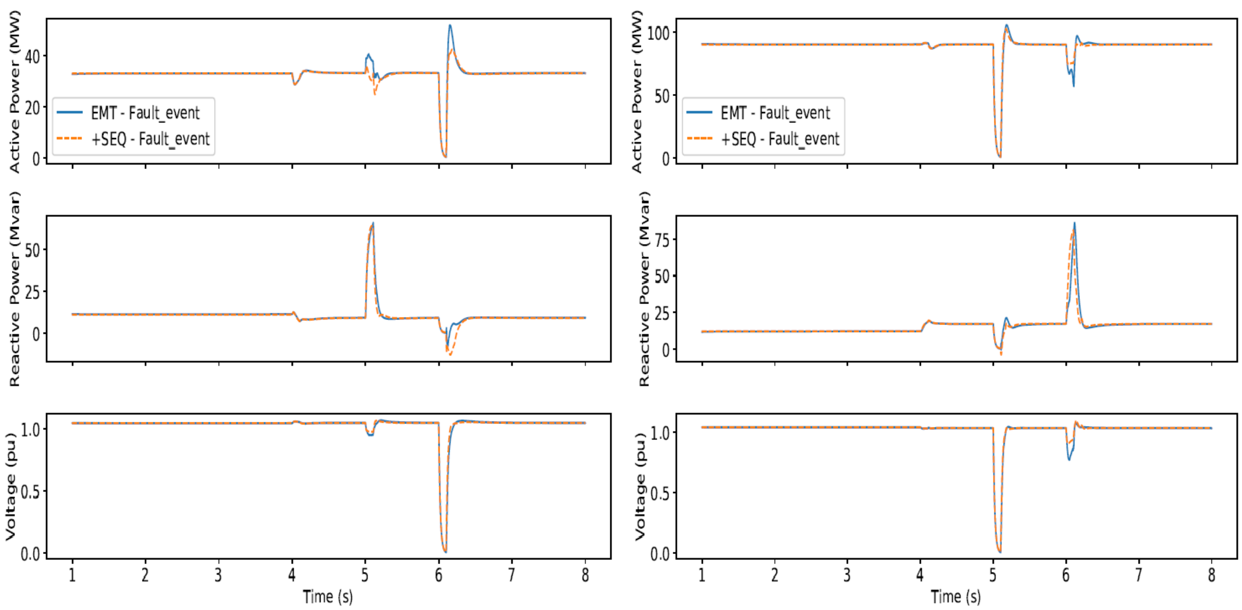

Figure 9: Behavior of IBR at bus 1 (left) and IBR at bus 2 (right) in response to multiple line outages followed by consecutive three phase to ground solid faults

<u>Benchmarking generic positive sequence model response against original equipment manufacturer (OEM) black box EMT model</u>

To further verify the behavior of the generic GFM positive sequence model for non-black start scenarios (as positive sequence simulations are not expected to be carried out for black start studies), the response of the generic model in PLL mode is compared against an OEM black box EMT model for a system islanding event. The reason for using the PLL mode here in this analysis is because the OEM model uses a combination of grid following control structure along with a virtual machine mode to bring about grid forming dynamics [9] both during a system interconnected operation and during subsequent islanded operation. It is again noted that in this scenario, a black start setup is not considered. The dynamic response for a disconnection of the system equivalent (resulting in a 100% IBR network) is shown in Figure 10.

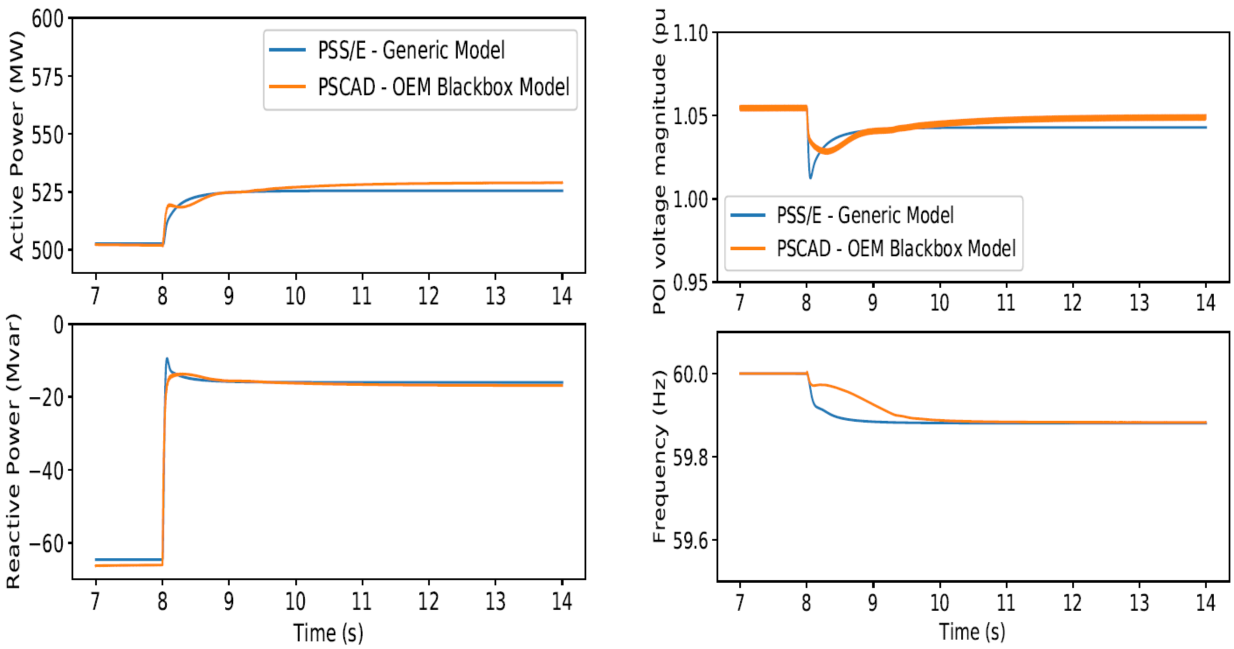

Figure 10: Dynamic response of positive sequence generic model behavior in PLL mode compared against OEM black box EMT model for system islanding event

The comparison of model behavior across both simulation domains, and a comparison of a generic positive sequence model with an OEM black box EMT model provides encouraging results regarding the validity of the university generic model. It is acknowledged that continuous validation studies with OEM models is to be carried out to keep the generic models up-to-date. However, with this generic model, transmission planners can begin to evaluate the behavior of grid forming IBR devices in their networks.

Numerical robustness in practical power system base cases

The numerical robustness of the model in practical bases cases has been verified and previously presented [10] [11] and is documented in [12] (in press). Here, two practical cases have been considered: (i) a portion of the Eastern Interconnection converted into a 100% IBR network with few fictitious modifications, and (ii) a small island system.

To further evaluate the robustness of the model, a large WECC system study was carried out. In this effort, an entire area of the WECC system was converted to a 100% IBR network. In the base case, this area has a mix of synchronous machine models (represented by GENROU, GENTPF, and GENTPJ) and IBR models (represented by a mix of 1st generation and 2nd generation WECC generic models). In the base case 70% (by rating) of the online generation in the area is represented by these synchronous machine models. To evaluate the robustness of the proposed generic GFM model, all synchronous machines in the area were replaced with the generic model, with equal rating/headroom. This results in a 100% IBR area with a mix of GFM and grid following IBRs in the same area. For the GFM resources, all four control methods were utilized and were assigned in a random fashion.

The event applied is the trip of 60% of the lines that connect this area to the rest of the interconnection. This results in reduction of the short circuit strength of the area in which the IBRs are connected. The trajectory of voltage and frequency as observed on a transmission bus at the area boundary is shown in Figure 11 and Figure 12 respectively. The blue curve corresponds to the base case (with synchronous machines in the area) while the red curve corresponds to the scenario with all synchronous machines in the area replaced with the generic GFM model. With the reduction in short circuit strength, and the change in flow of power due to trip of the interconnecting tie lines, in the base case, the synchronous machines are unable to survive due to reduction of damping torque. However, with the GFM resources, since there are no mechanical time constants involved, the system can settle to an acceptable value of voltage with no deviation in frequency.

In both simulations, no numerical robustness issues were observed. This study showcases the ability to successfully use multiple instances of the same generic GFM model in a base case as large as the WECC base case.

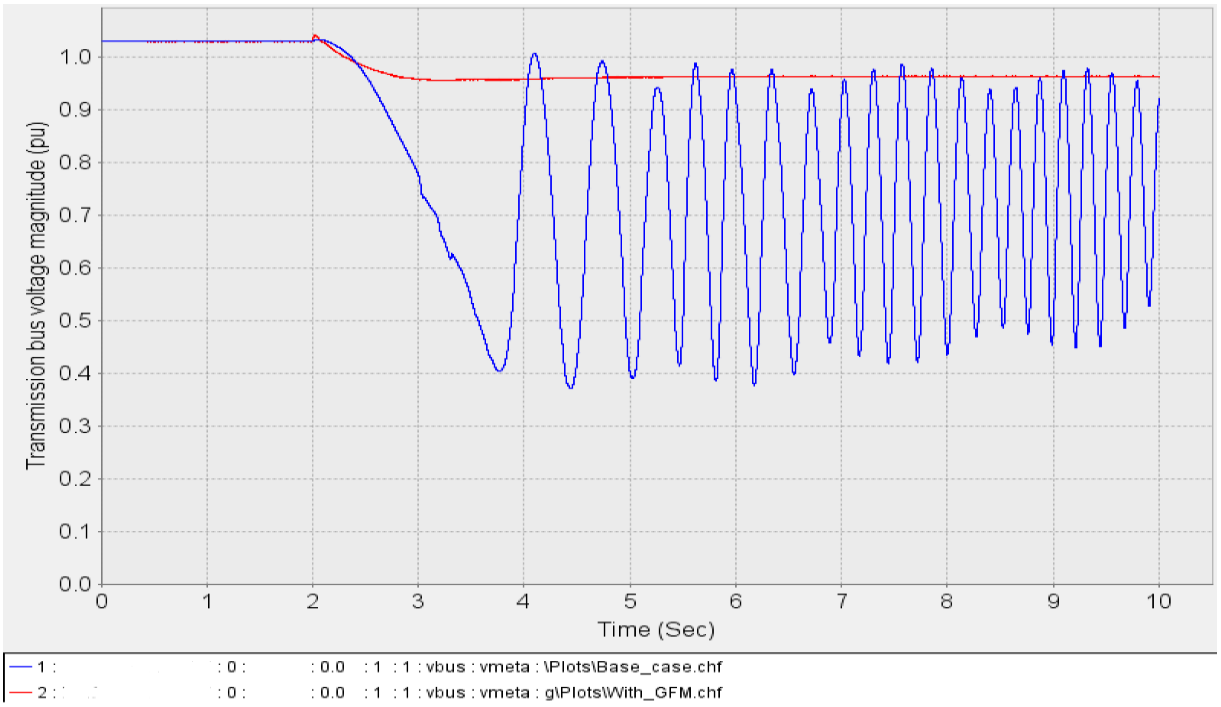

Figure 11: Voltage magnitude at transmission bus at the boundary of an area for an event disconnecting 60% of tie lines of the area (blue curve is base case with synchronous machines, red curve is with generic GFM model)

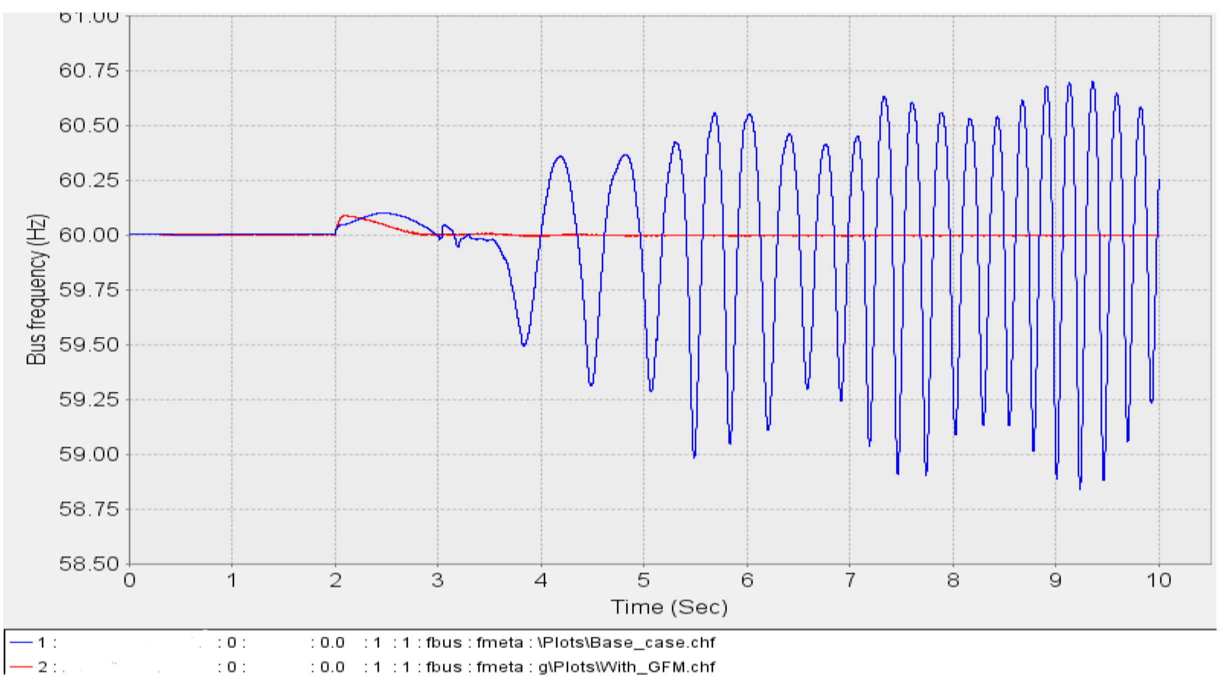

Figure 12: Bus frequency at transmission bus at the boundary of an area for an event disconnecting 60% of tie lines of the area (blue curve is base case with synchronous machines, red curve is with generic GFM model)

Acknowledgements
The development of this generic GFM model and its performance validation was supported, in part, by the U.S. Department of Energy, Solar Energy Technologies Office under Award Number DE-EE0009025 *A Scalable Control Architecture for 100% PV Penetration with Grid Forming Inverters* and, in part, by EPRI's Research Program 173: Bulk System Integration of Renewables and Distributed Energy Resources.

References

[1] B. Johnson, T. Roberts, O. Ajala, A. D. Dominguez-Garcia, S. Dhople, D. Ramasubramanian, A. Tuohy, D. Divan and B. Kroposki, "A Generic Primary-control Model for Grid-forming Inverters: Towards Interoperable Operation & Control," in *2022 55th Hawaii International Conference on System Sciences (HICSS)*, Maui, HI, USA, 2022.

[2] O. Ajala, N. Baeckeland, S. Dhople and A. D. Dominguez-Garcia, "Uncovering the Kuramoto Model from Full-order Models of Grid-forming Inverter-based Power Networks," in *IEEE Control and Decision Conference*, 2021.

[3] D. Ramasubramanian, "Differentiating between plant level and inverter level voltage control to bring about operation of 100% inverter-based resource grids," *Electric Power Systems Research [under review]*.

[4] D. Ramasubramanian and E. Farantatos, "Representation of Grid Forming Virtual Oscillator Controller Dynamics with WECC Generic Models," in *2021 IEEE PES General Meeting*, Washington D.C., USA, 2021.

[5] D. Ramasubramanian, P. Pourbeik, E. Farantatos and A. Gaikwad, "Simulation of 100% Inverter-Based Resource Grids With Positive Sequence Modeling," *IEEE Electrification Magazine,* vol. 9, no. 2, pp. 62-71, 2021.

[6] D. Ramasubramanian, W. Wang, P. Pourbeik, E. Farantatos, A. Gaikwad, S. Soni and V. Chadliev, "Positive Sequence Voltage Source Converter Mathematical Model for Use in Low Short Circuit Systems," *IET Generation, Transmission & Distribution,* vol. 14, no. 1, pp. 87-97, 2020.

[7] D. Ramasubramanian, A. Gaikwad, E. Farantatos and P. Pourbeik, "A Method of Implementation of Current Limits in REGC_B and REGC_C," 4 March 2019. [Online]. Available: https://www.wecc.org/Reliability/Memo%20on%20EPRI's%20method%20for%20implementation%20of%20current%20limit%20logic%20in%20REGC_B_C.pdf. [Accessed 3 November 2021].

[8] Electric Power Research Institute, "EMT and Positive Sequence Domain Model of Grid Forming PV Plant (GFM-PV)," EPRI, Palo Alto, CA, 2021, 3002021787.

[9] "Tesla Energy Software," Tesla, November 2021. [Online]. Available: https://www.tesla.com/support/energy/tesla-software. [Accessed November 2021].

[10] D. Ramasubramanian, "Simulation of 100% IBR grids with positive sequence modeling," August 2021. [Online]. Available: https://www.wecc.org/_layouts/15/WopiFrame.aspx?sourcedoc=/Administrative/Ramasubramanian%20-%20Simulation%20of%20100%20IBR%20Grids%20with%20Positive%20Sequence%20Modeling.pdf&action=default&DefaultItemOpen=1. [Accessed November 2021].

[11] D. Ramasubramanian, "Modeling of grid forming (GFM) IBR and frequency response in a 100% IBR Grid," October 2021. [Online]. Available: https://www.wecc.org/_layouts/15/WopiFrame.aspx?sourcedoc=/Administrative/WECC%20Grid%20Forming%20Inverter%20Based%20Resources%20.1.pdf&action=default&DefaultItemOpen=1. [Accessed November 2021].

[12] Electric Power Research Institute, "Grid Forming Inverters for Increase in Inverter Based Resource Percentage," EPRI, Palo Alto, CA, 2021, 3002020786.